Electronic supplementary information

White circularly polarized luminescence from dual - component emitter induced by FRET between tetraphenylene and PDI derivatives

Huanhuan Dong [a], Huajing Li [a], Enquan Tian [b], Yijun Zhang [a], Jian Kong [a], Yuangang Li*[a]

a. College of Chemistry and Chemical Engineering, Xi'an University of Science and Technology, Xi'an 710054, China E-mail: Liyuangang@xust.edu.cn
b. College of Materials Science and Engineering, State Key Laboratory of Bio-fibers and Eco-textiles, Shandong Collaborative Innovation Center of Marine Biobased Fibers and Ecological Textiles, Qingdao University, Qingdao, 266071, China

Experimental Procedures

Materials

L-Aspartic acid and D-Aspartic acid were purchased from Shanghai District of Japan TCI Co. Ltd. and GLS Co. Ltd., respectively. N-Hydroxysuccinimide (NHS, $C_4H_5NO_3$) and 4- (1,2,2-triphenylvinyl) benzoic acid were bought from Aladdin Chemical Reagent Co. Ltd. Furthermore, 1-(3-Dimethylaminopropyl)-3-ethylcarbodiimide hydrochloride (EDC•HCl), and N,N-Dimethylformamide (DMF,99.9%) were purchased from Innochem Co. Ltd. In addition, Ethanol absolute (C_2H_5OH) was purchased from Guangdong Guanghua Sci-Tech Co. Ltd. (99.7%). The other solvents were provided by China Tianjin Fuyu Fine Chemical Co. Ltd., and all the chemicals available were used directly without further purification.

Characterization

NMR Spectroscopy

^{1}H and ^{13}C nuclear magnetic resonance (NMR) spectra were recorded on a Bruker Avance III spectrometer using C_2D_6SO as solvent. MeSi was used as an internal standard. The chemical shifts are reported in ppm, referring to the proton signal of the solvent as an internal standard. The multiplicities of the proton signal are denoted as follows: s = singlet, d = doublet, t = triplet, q = quartet, quin = quintuplet, m = multiplate, respectively.

Fluorescence Spectroscopy.

The fluorescence spectra were recorded on a HORIBA Instruments Duetta fluorescence spectrometer and corrected for photomultiplier and lamp intensity. Liquid samples were held in a 1 cm light range quartz cuvette with a 90°angle of the beam from the light source to the detector and a liquid concentration less than or equal to 10^{-4} mol·L^{-1}. The excitation wavelength is 370 or 495 nm and the slit width

can be set to 3 nm or 5 nm depending on the sample. The fluorescence quantum yields are measured in a HAMAMATSU quantum yield measurement system. The external light source was a continuous xenon lamp E7536 (Japan). The spectrum data is the average of three measurements. The excitation wavelength range was 370 or 495 nm.

UV/Vis Spectroscopy.

The UV/Visible absorption spectra were recorded using a Shimadzu UV-2600 UV-Vis spectrophotometer. The spectra were measured in the ultraviolet region of dilute solutions using a quartz cuvette with an optical range of 1 cm and deionized water prepared by the UPP Pure Water Preparation System UPH-1-60 L. The concentration of the solution was less than or equal to 10^{-4} mol·L^{-1}.

SEM

The micro-morphology of the materials at different scales was recorded using the scanning electron microscope of Phenom/Pro from Fina, the Netherlands, at an accelerating voltage of 10 kV. Prior to testing: (i) dilute the sample until it is completely dissolved; (ii) gently fish out the solute from the solution with a carbon film copper mesh while heating to 80℃; and (iii) allow it to dry in the air before testing.

DLS

DLS measurements were made at room temperature on a Malvern Potentiometric Laser Nanoparticle Sizer, model ZEN3690, using a 10 mm Hellma quartz glass cuvette. DLS was measured on Malvern, zeta sizer, model ZEN3690 at 25℃.

CD

The CD spectra were recorded using a quartz cuvette of 0.1 mm path length in a JASCO-J-815 spectropolarimeter under a nitrogen atmosphere at room temperature.

CPL

The CPL spectra were recorded using a JASCO-CPL-810 spectrometer, and the excitation/emission wavelengths for the CPL spectra were 370 nm.

Synthetic Routes and Structural Characterizations

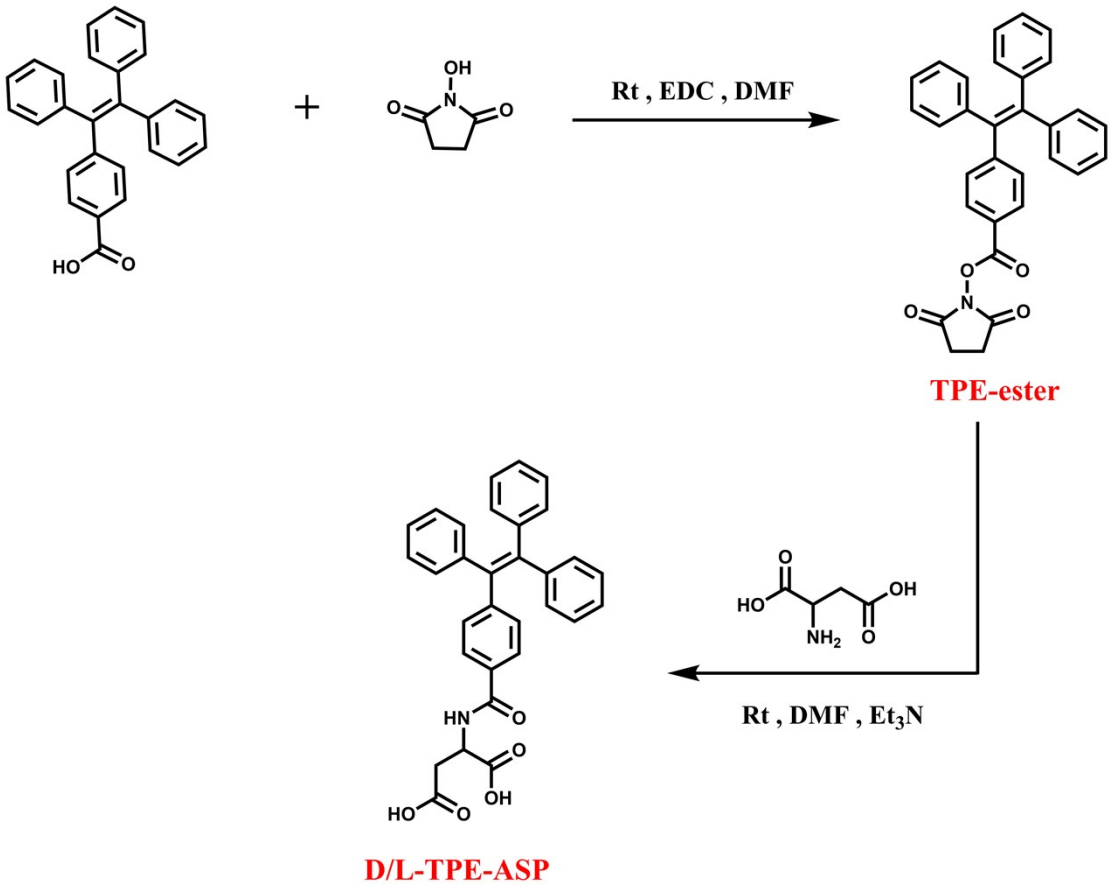

Scheme S1. Synthetic routes of TPE-ASP.

Synthesis of TPE-ester

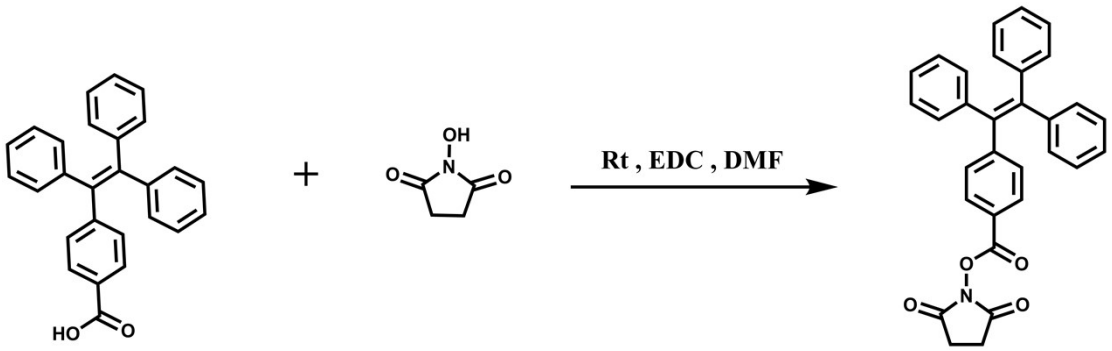

Scheme S2. Synthetic routes of TPE-Ester.

4- (1,2,2-triphenylvinyl) benzoic acid (752.9 mg, 2 mmol), N-hydroxysuccinimide (NHS, 460.4 mg, 4 mmol) and 1-(3-Dimethylaminopropyl)-3-ethylcarbodiimide hydrochloride (EDC·HCl, 766.8 mg, 4 mmol) were dissolved in ultra-dry DMF (35 mL). The mixture was stirred at room temperature for 72 hours in a 100 mL flask. After the reaction was completed, the solvent was removed, and the residue was dissolved in a small amount of acetone. After adding 1M hydrochloric acid, white flocs were precipitated. After filtration and washing, the final product was obtained. After vacuum drying, the white solid powder (recorded as : TPE-ester) was 812 mg, and the yield was 85.7 %.**^{1}H NMR** (400 MHz, DMSO-d_6) δ 7.86 (d, J=12.4 Hz, 2H), 7.22 (d, J = 6.8 Hz, 2H), 7.21-7.00 (m, 12H), 7.00-6.95 (m, 3H), 2.50-2.49 (m, 4H).**^{13}C NMR** (101 MHz, DMSO-d6) δ 170.8, 161.9, 151.3, 143.2, 143. 0, 142.9, 142.7, 139.7, 132.2, 131.2, 131.1, 130.1, 128.6, 128.6, 128.4, 127.7, 127.6, 122.6, 26.0.

Synthesis of L-TPE-ASP

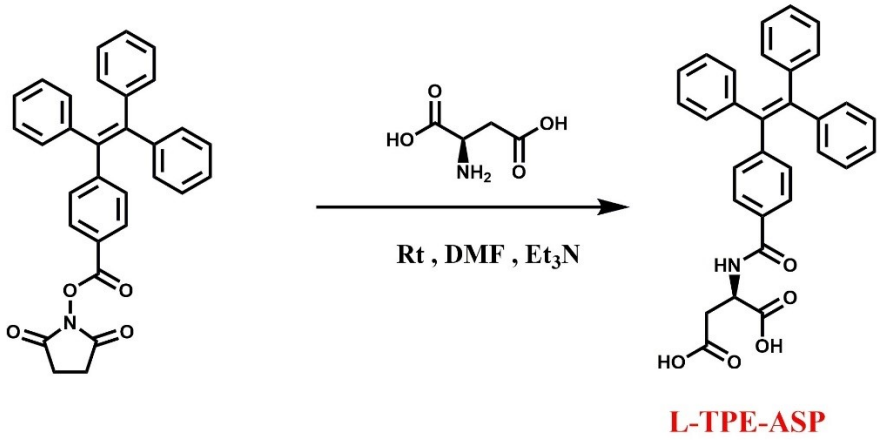

Scheme S3. Synthetic routes of L-TPE-ASP.

TPE-ester (400 mg,0.845 mmol), (170 mg, 1.26 mmol), ultra-dry triethylamine (TEA, 630 μL, 458.9 mg, ρ = 0.728) were dissolved in ultra-dry DMF (45 mL). The mixture was stirred at room temperature for 72 hours in a 100 mL flask. After the reaction is completed, the solvent is removed, and the residue is dissolved in a small amount of acetone. After adding 1M hydrochloric acid, floccules are precipitated, white products are obtained after filtration and washing, and white solid powder is obtained after vacuum drying. The solid powder was crystallized, filtered and washed in a mixed solution of n-hexane and dichloromethane (DCM). After vacuum drying, a white solid powder with high purity of 357 mg was obtained, which was the final product, recorded as L-TPE-ASP, with a yield of 85.9 %.**^{1}H NMR** (400 MHz, DMSO-d_6) δ 14.01 – 11.47 (m, 1H), 8.62 (d, J = 7.8 Hz, 1H), 7.62 (d, J = 8.4 Hz, 2H), 7.18 – 6.97 (m, 17H), 4.69 (td, J = 7.9, 5.7 Hz, 1H), 2.81 (d, J = 22.2 Hz, 1H), 2.65 (d, J = 16.4 Hz, 1H). **^{13}C NMR** (101 MHz, DMSO-d_6) δ 173.1, 172.3, 166.1, 147.1, 143.4, 143.2, 142.0, 140.3, 132.1, 131.2, 131.1, 128.5, 128.4, 128.3, 127.4, 127.4, 127.2, 49.8, 36.4.

Synthesis of D-TPE-ASP

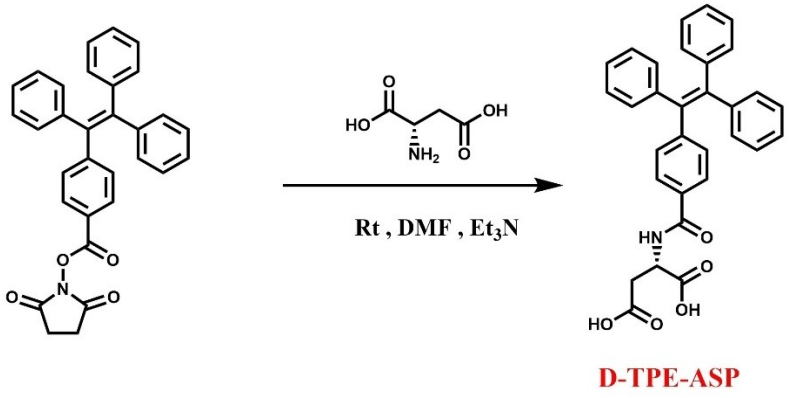

Scheme S4. Synthetic routes of D-TPE-ASP.

TPE-ester (200 mg,0.42 mmol), D-Aspartic acid (83 mg, 0.63 mmol), ultra-dry triethylamine (TEA, 315 μL, 229.5 mg, ρ = 0.728) were dissolved in ultra-dry DMF (30 mL). The mixture was stirred at room temperature for 72 hours in a 100 mL flask. After the reaction is completed, the solvent is removed, and the residue is dissolved in a small amount of acetone. After adding 1M hydrochloric acid, floccules are precipitated, white products are obtained after filtration and washing, and white solid powder is obtained after vacuum drying. The solid powder was crystallized, filtered and washed in a mixed solution of n-hexane and dichloromethane (DCM). After vacuum drying, a white solid powder with high purity of 163 mg was obtained, which was the final product, recorded as D-TPE-ASP, with a yield of 78.9 %.**^{1}H NMR** (400 MHz, DMSO-d6) δ 12.70 (s, 2H), 8.63 (d, J = 7.8 Hz, 1H), 7.64-7.60 (m, 2H), 7.17-6.97 (m, 17H), 4.68 (td, J = 7.8, 5.8 Hz, 1H), 2.82-2.63 (m, 2H). **^{13}C NMR** (101 MHz, DMSO-d_6) δ 173.1, 172.3, 166.1, 147.1, 143.4, 143.2, 142.0, 140.3, 132.1, 131.2, 131.1, 128.5, 128.4, 128.3, 127.4, 127.4, 127.2, 49.8, 36.4.

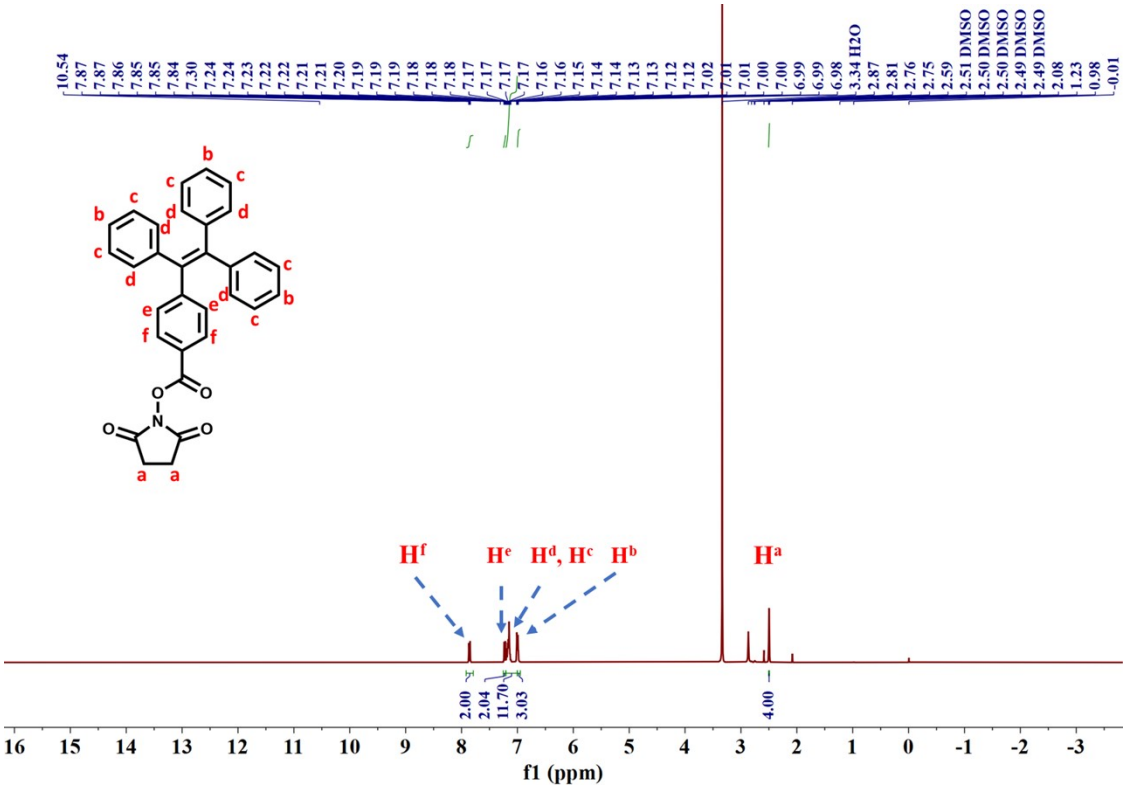

Fig. S1 ^{1}H NMR of TPE-ester.

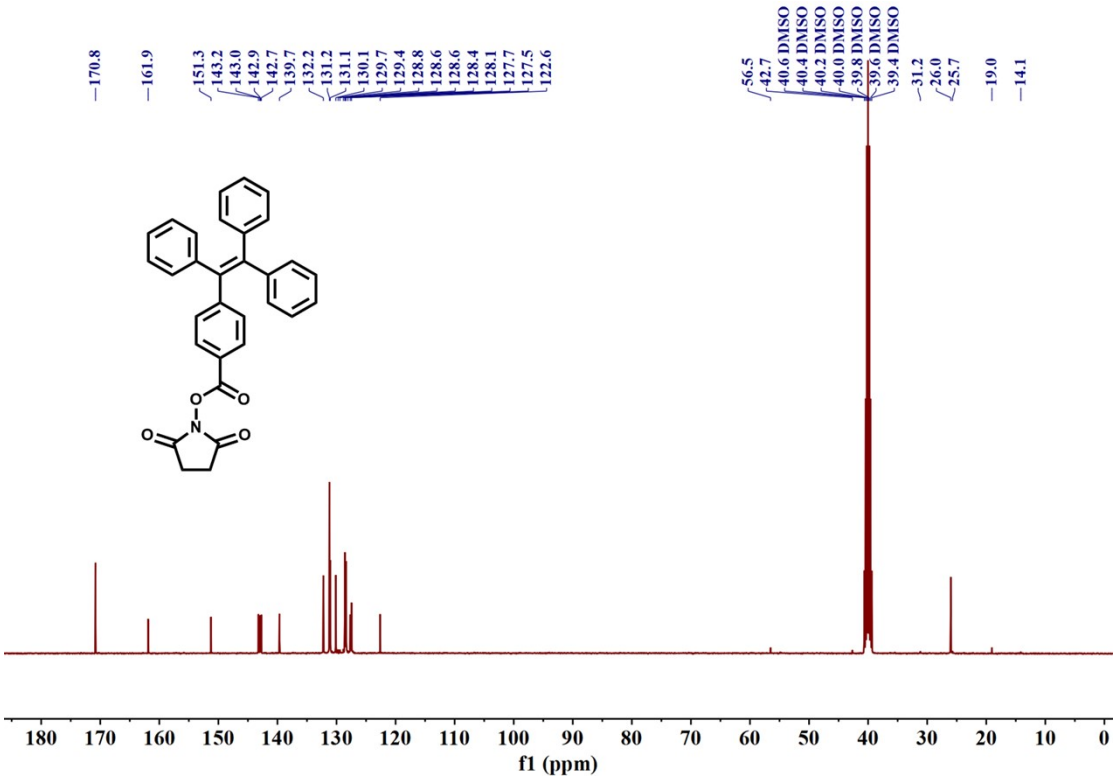

Fig. S2 ^{13}C NMR of TPE-ester.

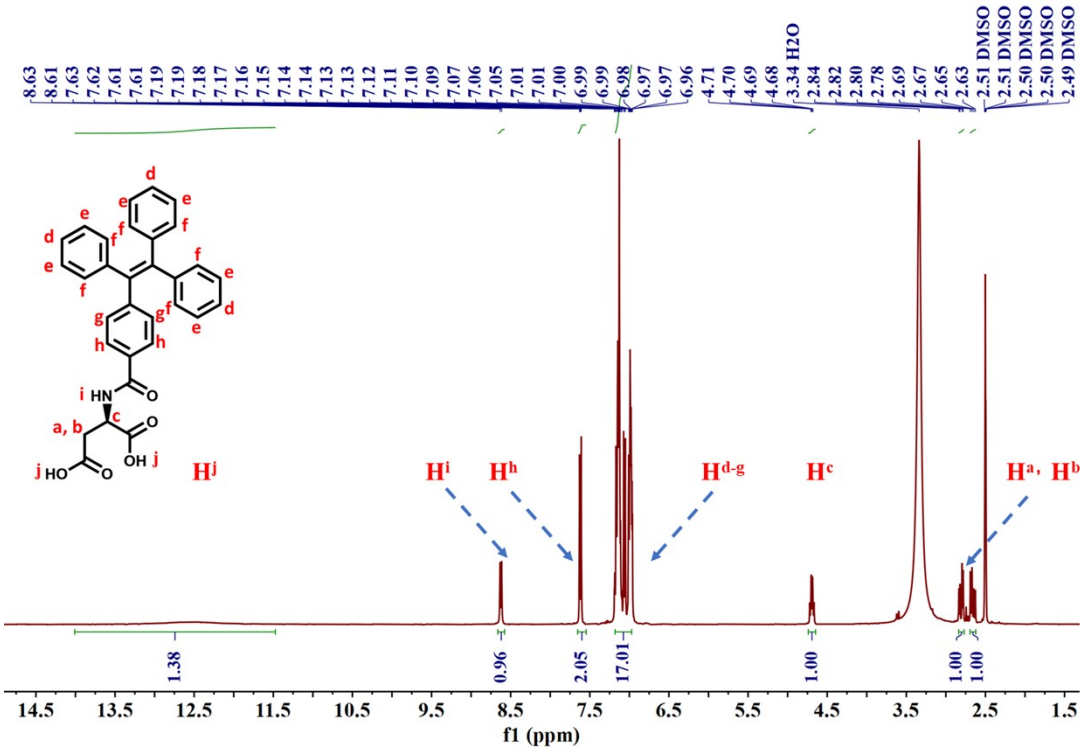

Fig. S3 ^{1}H NMR of L-TPE-ASP.

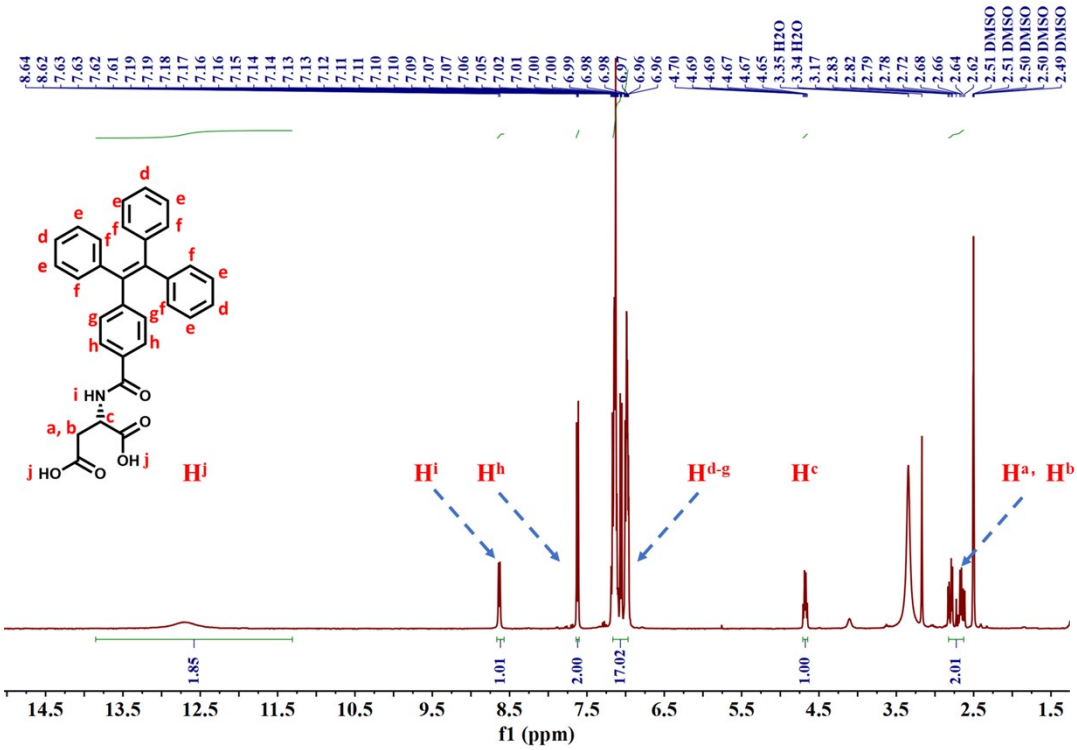

Fig.S4. ^{1}H NMR of D-TPE-ASP.

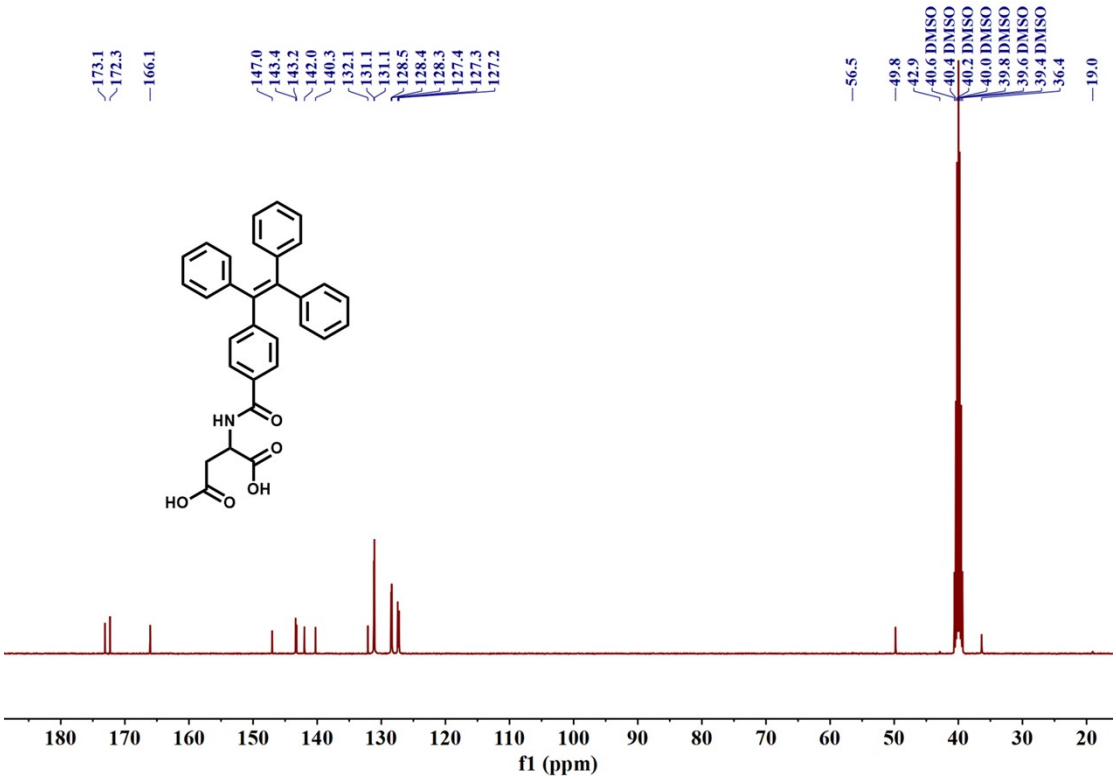

Fig. S5. ^{13}C NMR of TPE-ASP.

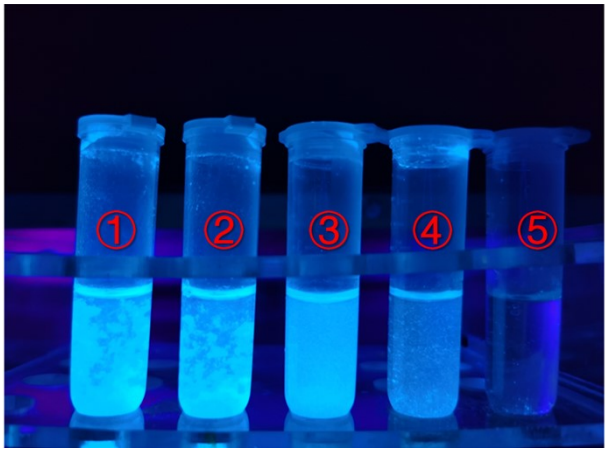

Fig. S6 The luminescence images of TPE-ASP assemblies with different concentrations when the ratio of water and dioxane is 9: 1 (the listed images are all after standing for 120 min, and the 365 nm handheld ultraviolet lamp is used as the excitation light source). The concentrations from ① to ⑤ are: 2×10^{-4} M, 1.5×10^{-4} M, 1×10^{-4} M, 5×10^{-5} M and 1×10^{-5} M.

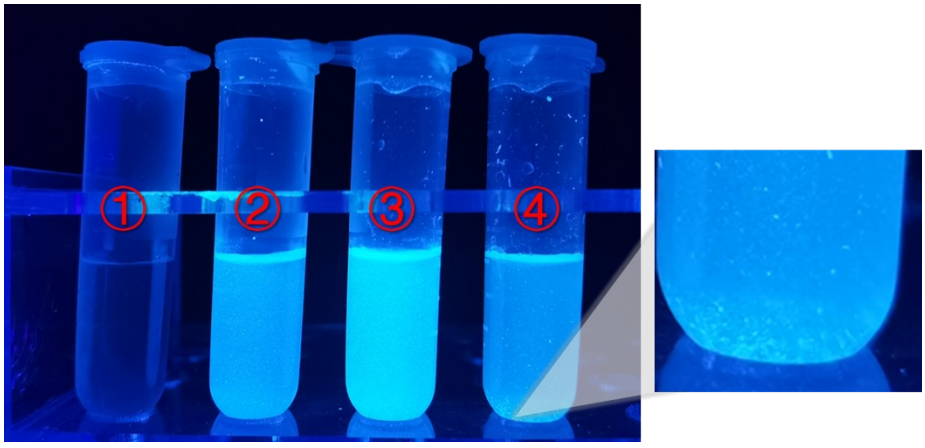

Fig. S7 The luminescence images of TPE-ASP assemblies under different water and dioxane ratios when the concentration of TPE-ASP is 10^{-4} M, (the listed images are all after standing for 120 min, and the 365 nm handheld ultraviolet lamp is used as the excitation light source). The proportions of dioxane and water in ① to ④are: 30:70, 20:80, 10:90 and 5:95.

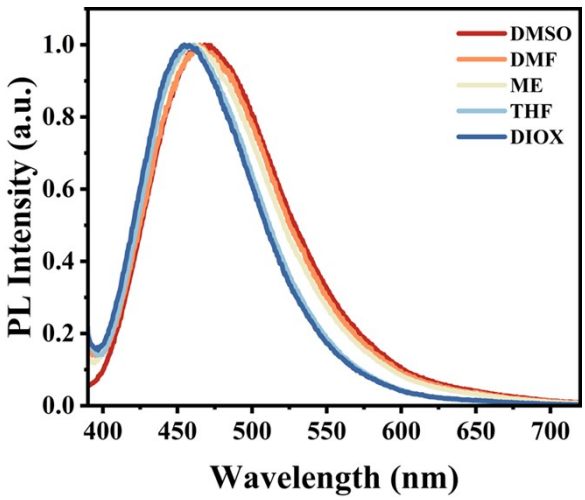

Fig. S8 Fluorescence emission spectra of TPE-ASP in different solvents.

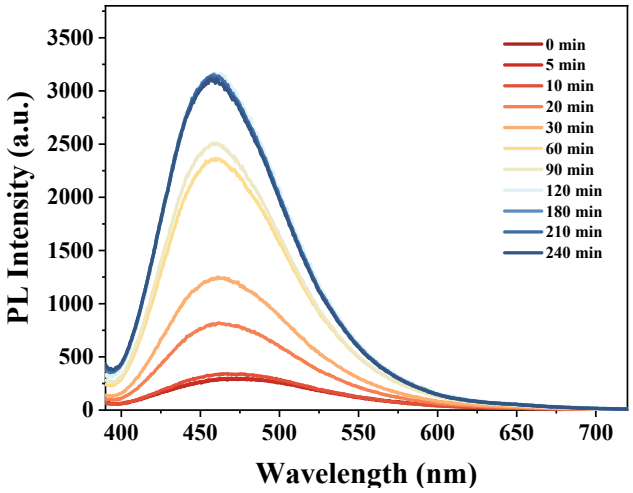

Fig. S9 Time-dependent fluorescence spectra of TPE-ASP.

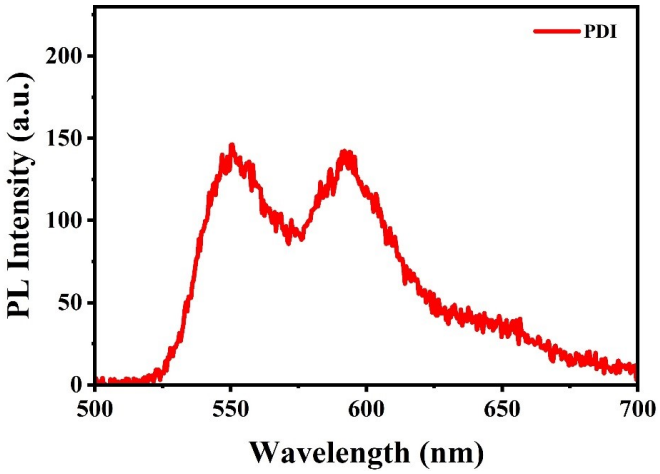

Fig. S10 Fluorescence Spectra of PDI (λ_{ex}= 495 nm).

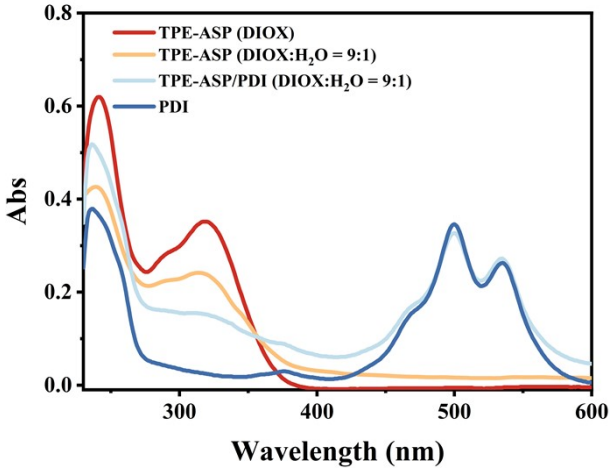

Fig. S11 Absorption spectra of monomers and assemblies. (The red line is the absorption spectrum of TPE-ASP in pure DIOX. The orange line is the absorption spectrum of TPE-ASP in mixed solvent (DIOX: H_2O = 1:9). The light blue line is the absorption spectrum of the co-assembly of TPE-ASP and PDI, and the dark blue line is the absorption spectrum of PDI.)

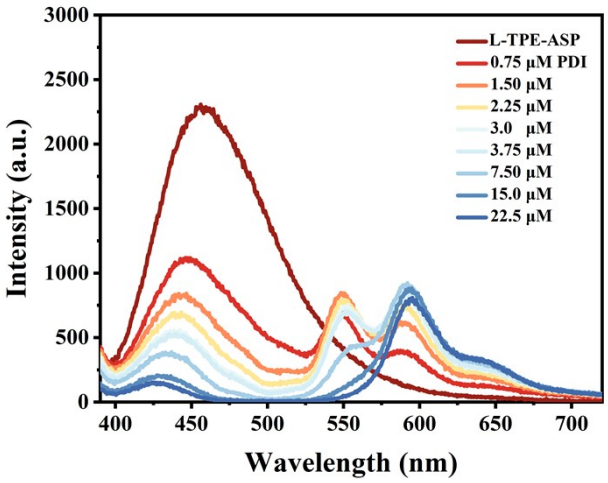

Fig. S12 Fluorescence Spectra PDI titration of L-TPE-ASP (10^{-4} M) in H_2O-DIOX (9/1, V/V), λex = 370 nm

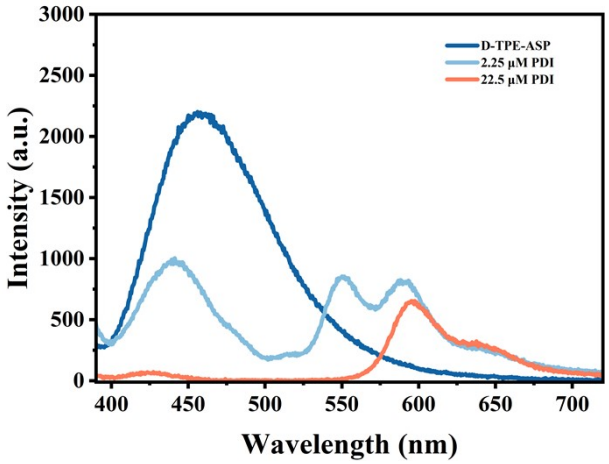

Fig. S13 Fluorescence Spectra PDI titration of D-TPE-ASP (10^{-4} M) in H_2O-DIOX (9/1, V/V), λex = 370 nm

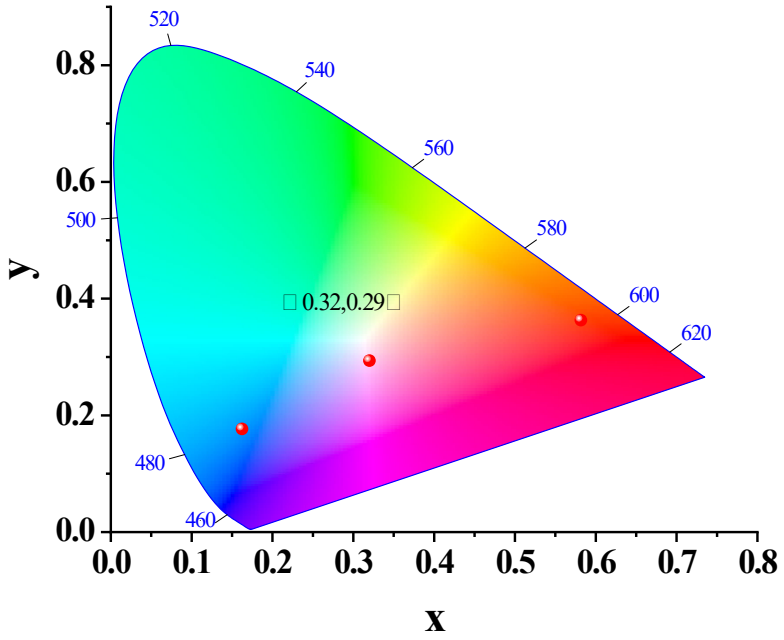

Fig. S14 CIE coordinate of D-TPE-ASP (10^{-4} M) in H_2O-DIOX (9/1, V/V), λex = 370 nm

The energy transfer efficiency and antenna effect of LHS constructed by TPE-ASP/PDI

According to the Eq. S1:

$$\Phi_{ET}=1-I_{DA}/I_{D} \qquad \text{S1}$$

Where I_{DA} and I_{D} are the fluorescence intensities at 460 nm of TPE-ASP/PDI and TPE-ASP respectively when directly excited at 370 nm.

According to the Eq. S2:

$$AE=(I_{DA,370}-I_{D,370})/I_{DA,495} \qquad \text{S2}$$

Where $I_{DA,370}$ and $I_{D,370}$ are the fluorescence intensities at 595 nm of TPE-ASP/PDI and PDI respectively when indirectly excited at 370 nm $I_{DA,495}$ is the fluorescence intensities at 595 nm of TPE-ASP/PDI when directly excited at 495 nm.

Tab. S1 Φ_{ET} calculation of L-TPE-ASP/PDI in H_2O-DIOX (9/1; V/V)

	D:A	$I_D(I_{DA})$	L-TPE-ASP/PDI $\Phi_{ET}(\%)$
		2306.28	
	100 : 0.75	1015.16	55.98
	100 : 1.50	819.26	64.48
	100 : 2.25	654.78	71.61
$\Phi_{ET}=1-I_{DA}/I_D$	100 : 3.00	546.5	76.30
	100 : 3.75	511.75	77.81
	100 : 7.50	371.96	83.87
	100 : 15.0	207.29	91.01
	100 : 22.5	136.04	94.10

Tab. S2 Φ_{ET} calculation of D-TPE-ASP/PDI in H_2O-DIOX (9/1; V/V)

	D:A	$I_D(I_{DA})$	D-TPE-ASP/PDI Φ_{ET} (%)
		2200	
$\Phi_{ET}=1-I_{DA}/I_D$	100 : 0.75	990	55.00
	100 : 2.25	399.67	81.83
	100 : 22.5	116.9	94.69

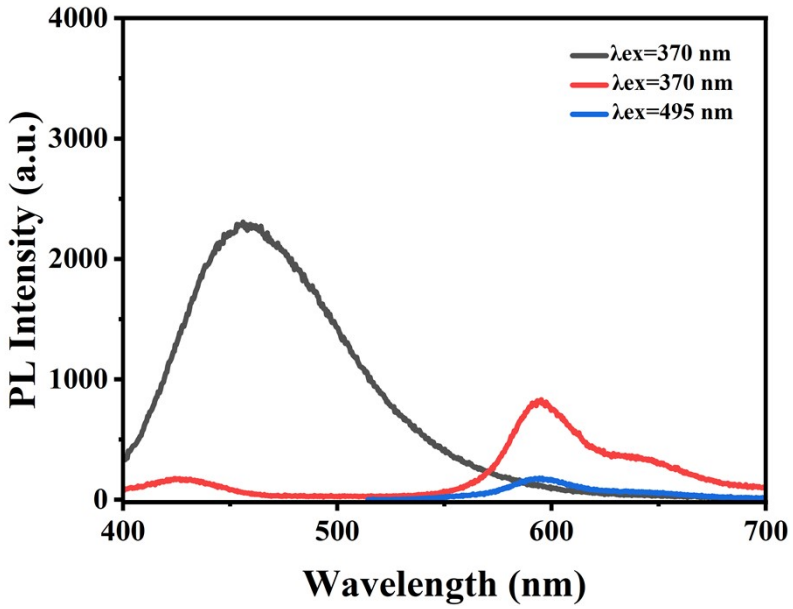

Fig. S15 Fluorescence Spectra of Antenna Efficiency Data of L-TPE-ASP/PDI System

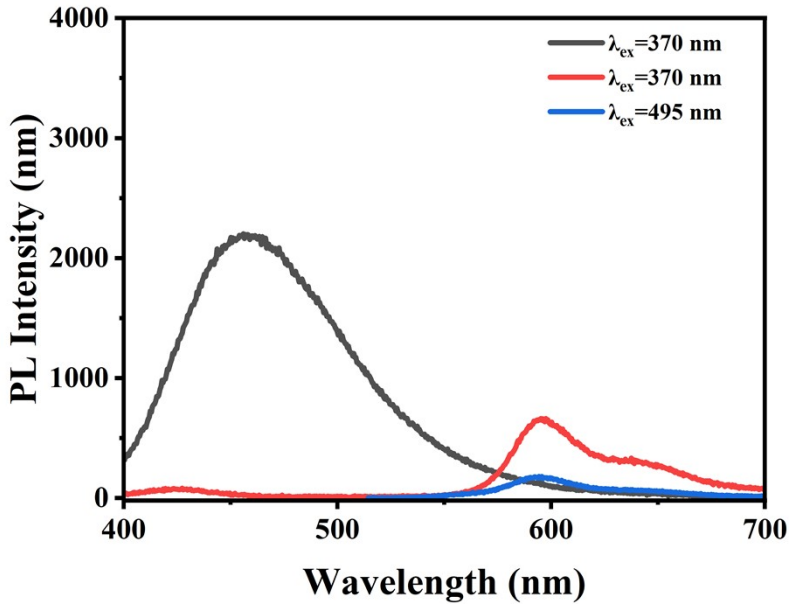

Fig. S16 Fluorescence Spectra of Antenna Efficiency Data of D-TPE-ASP/PDI System

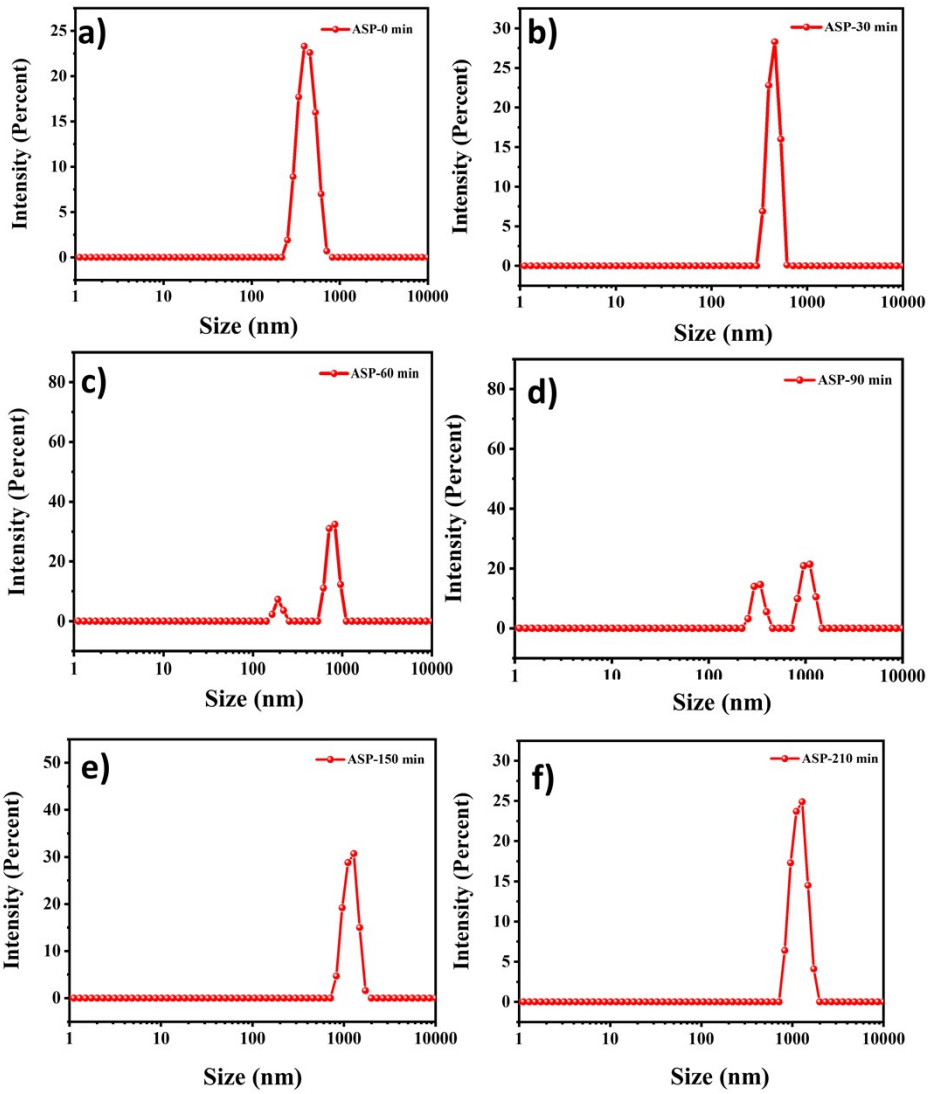

Fig. S17 DLS of the aggregation process of TPE-ASP assemblies。

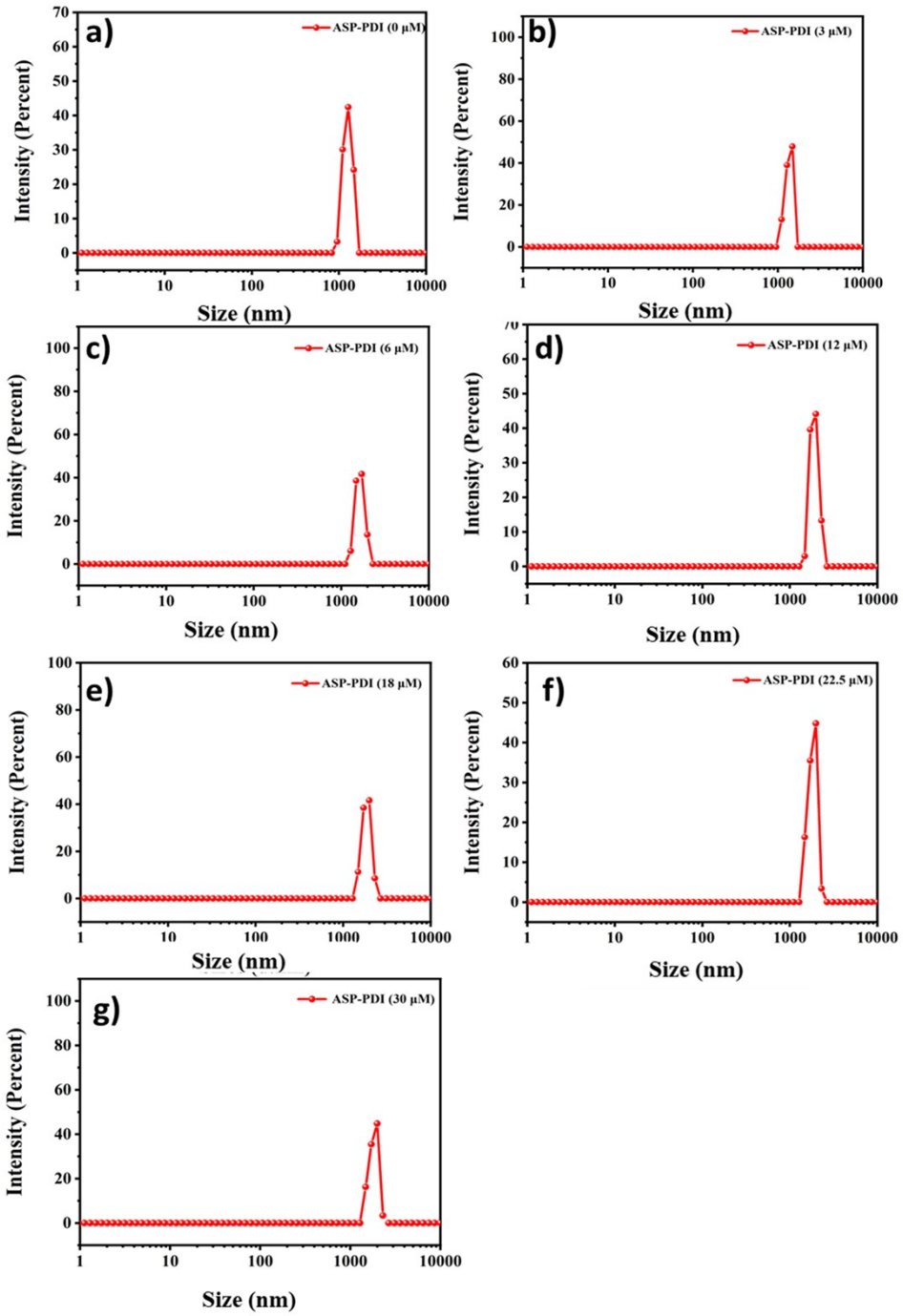

Fig. S18 DLS titration process of TPE-ASP/PDI

Tab. S3 Zeta potential of L-TPE-ASP/PDI in H_2O-DIOX (9/1; V/V)

ASP-PDI	Zeta Potential-1 /mV	Zeta Potential-2 /mV	Zeta Potential-3 /mV	Zeta Potential /mV
0	-28.1	-31.9	-30.9	-30.3
100:0.15	-13.9	-12.9	-12.9	-13.23
100:0.3	3.67	-0.944	-5.58	-0.951
100:0.45	1.92	2.78	3.43	2.71
100:0.6	17.9	8.87	2.79	9.85
100:0.75	16.3	9.73	10.1	12.04
100:1.5	16	14.8	14	14.93
100:2.25	18.9	18.6	16.8	18.1
100: 3	19.1	18.5	17.8	18.47
100: 6	21.1	19.7	19.1	19.97
100:12	19.5	20.6	17.1	19.07
100:22.5	20.6	20	17.5	19.37

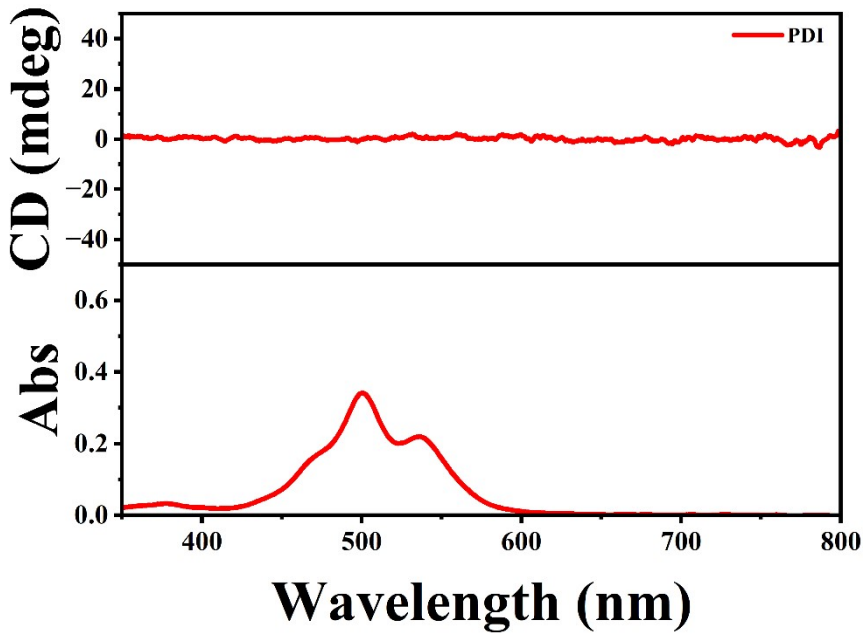

Fig. S19 CD Spectra of PDI.

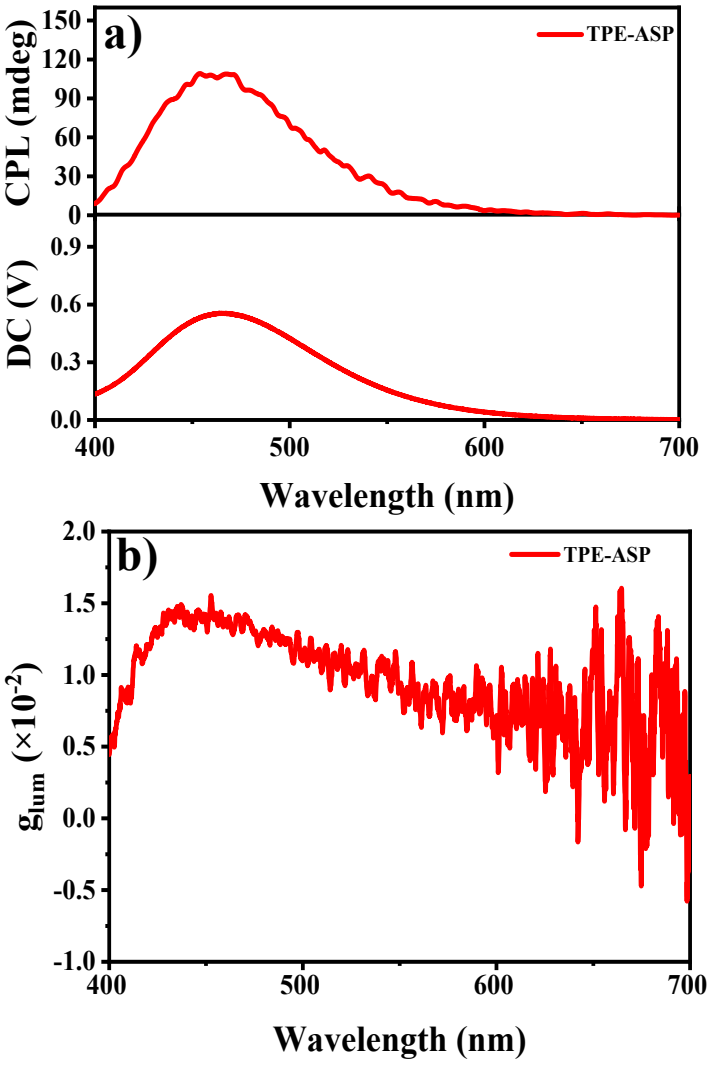

Fig. S20 a) CPL spectra and b) g_{lum} of simultaneous blending of of TPE-ASP/PDI .

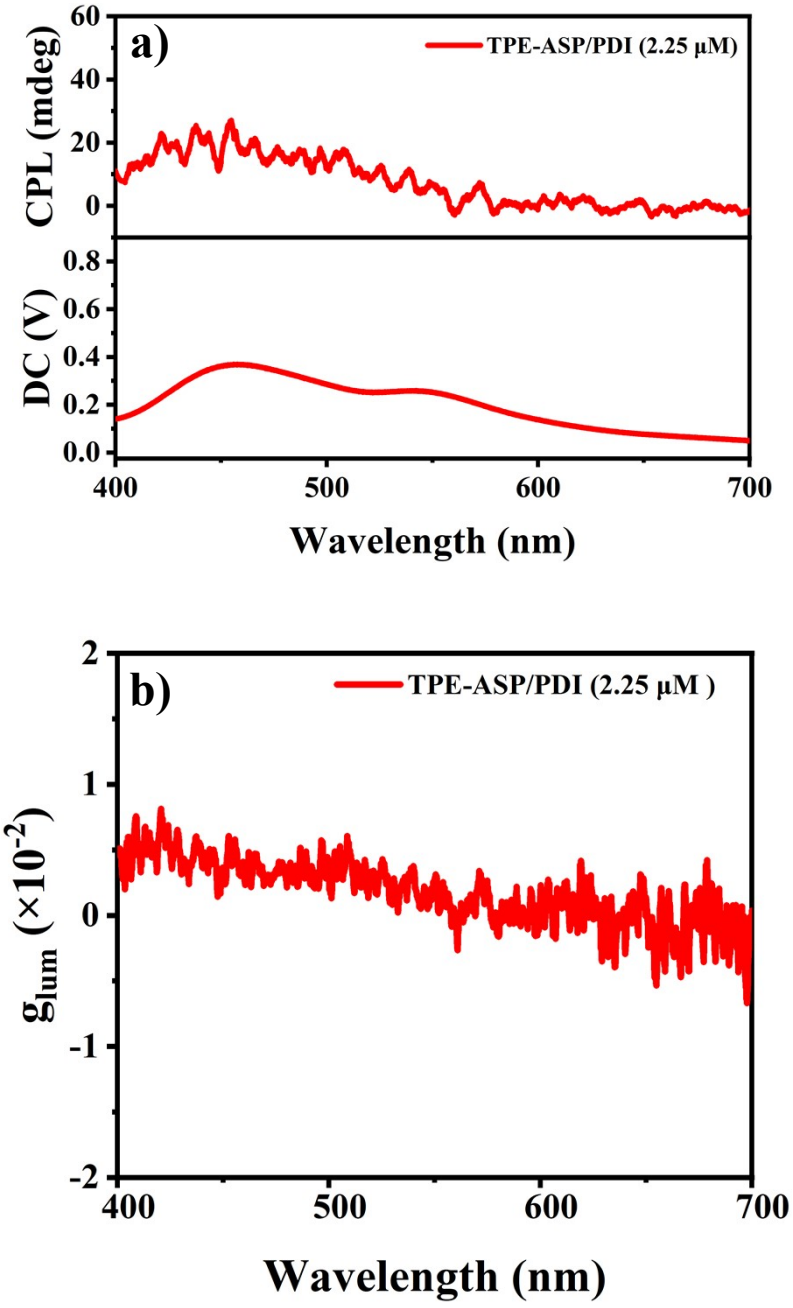

Fig. S21 a) CPL spectra and b) g_{lum} of simultaneous blending of of TPE-ASP/PDI (2.25 μM).

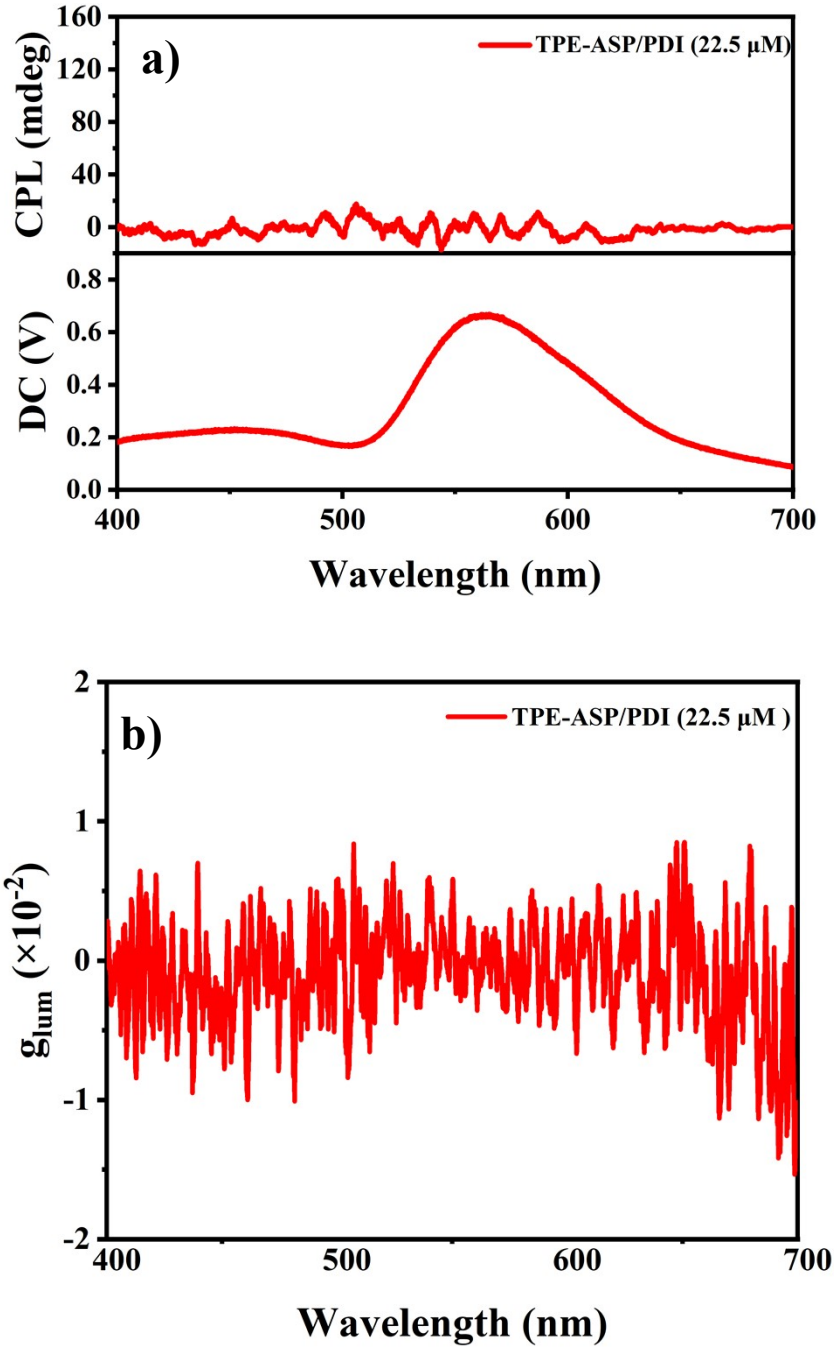

Fig. S22 a) CPL spectra and b) g_{lum} simultaneous blending of of TPE-ASP/PDI (22.5 μM).

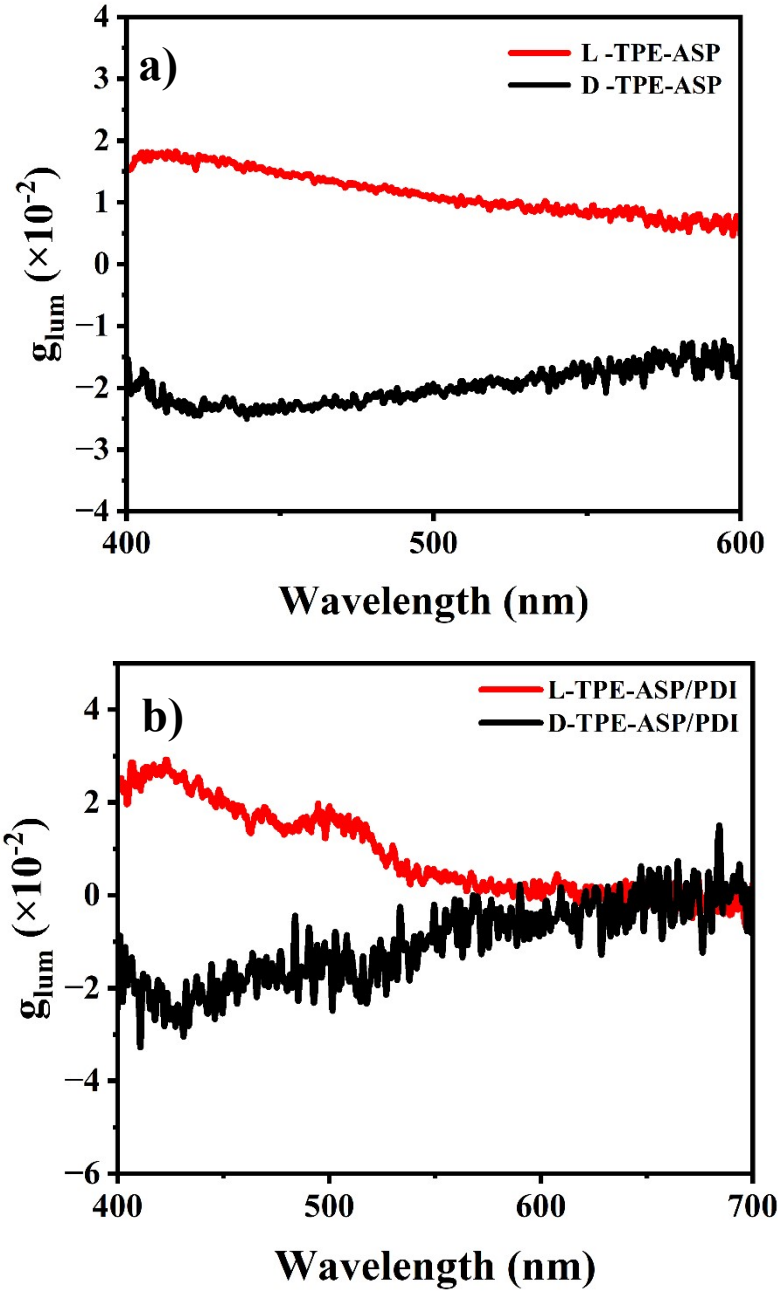

Fig. S23 g_{lum} of a) L-/D-TPE-ASP and L-/D-TPE-ASP-PDI (22.5 μM).

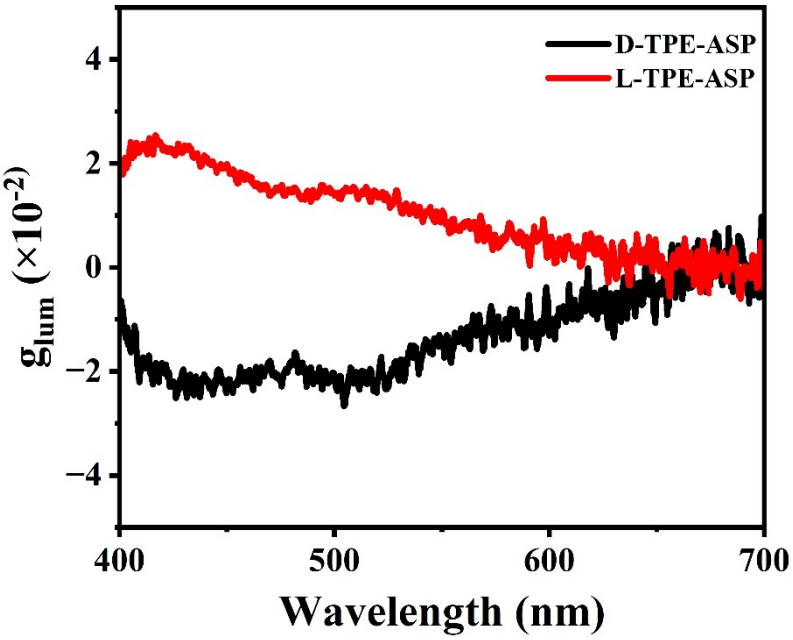

Fig. S24 g_{lum} of a) L-/D-TPE-ASP and L-/D-TPE-ASP-PDI (2.25 μM)

For the construction of the FRET process, we used two assembly methods, namely monodisperse TPE-ASP and PDI co-assembly, and fully assembled TPE-ASP and PDI co-assembly. These two methods are evaluated by CPL detection. Fig. S18-20 shows the first case mentioned above. Obviously, under this condition, the CPL signal of the system decreases with the increase of PDI. When the assembled TPE-ASP is co-assembled with PDI (Fig. S21, S22), we observe the enhancement of chiral signal and the increase of g value. Therefore, our FRET process is based on the formation of TPE-ASP assembly first and then co-assembly with PDI.

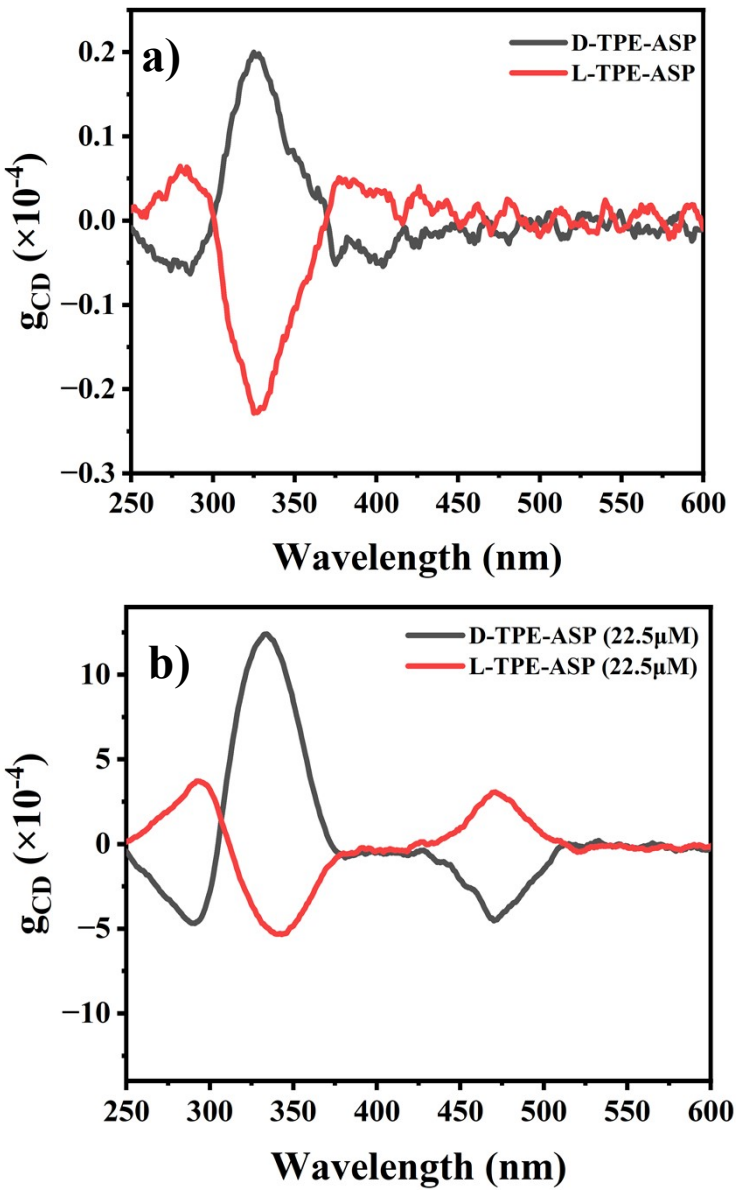

Fig. S25 g_{abs} of a) L-/D-TPE-ASP and L-/D-TPE-ASP-PDI (22.5 μM)

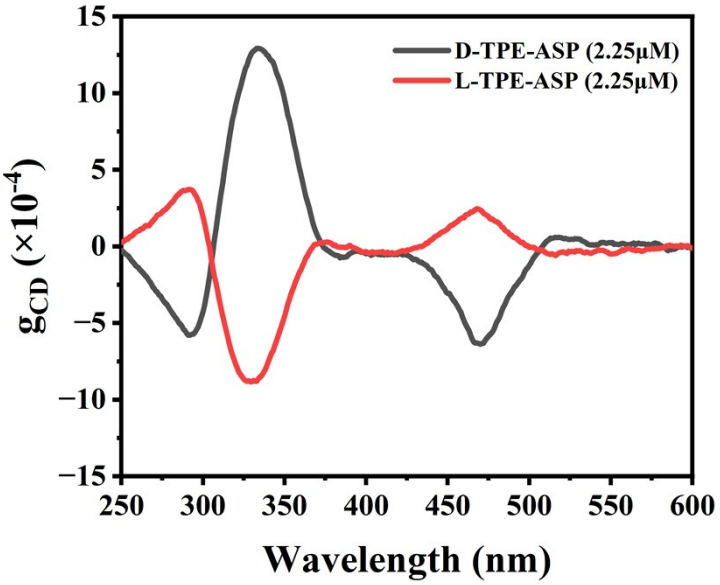

Fig. S26 g_{abs} of a) L-/D-TPE-ASP and L-/D-TPE-ASP-PDI (2.25 μM)

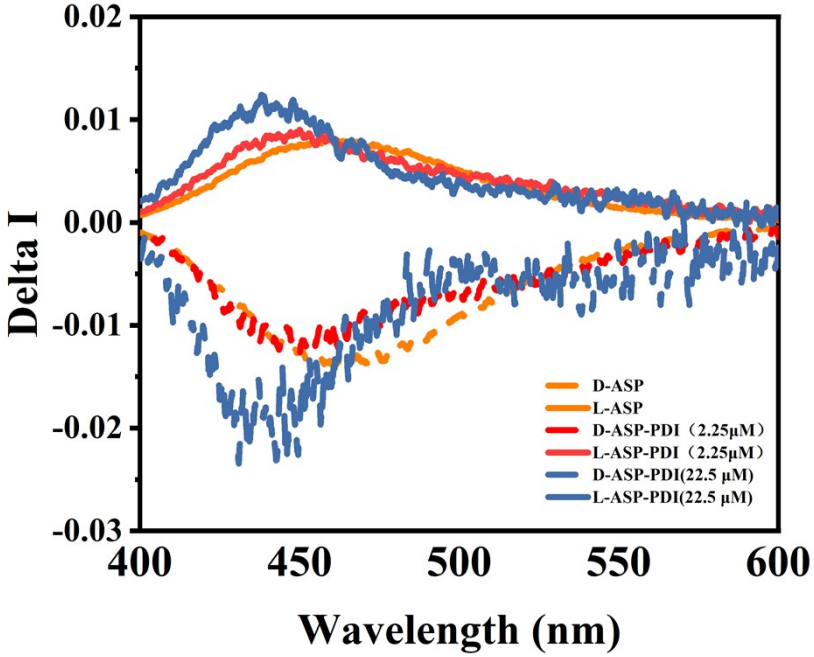

Fig. S27 Delta I of the assembly

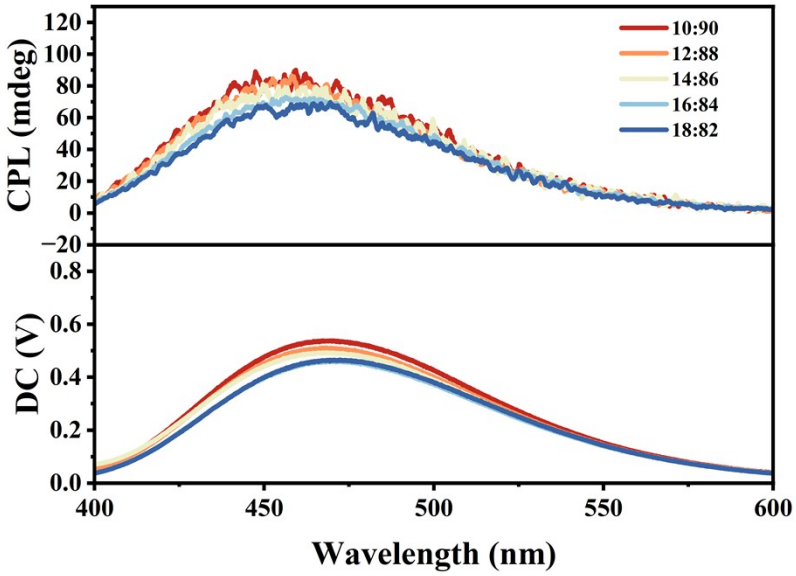

Fig. S28 CPL with different solvent ratios

Tab. S4 g_{abs} of TPE-ASP/PDI in H_2O-DIOX (9/1; V/V)

340nm			
D-TPE-ASP	0.19×10^{-4}	L-TPE-ASP	-0.22×10^{-4}
D-TPE-ASP/PDI (2.25μM)	12.91×10^{-4}	L-TPE-ASP/PDI (2.25μM)	-8.76×10^{-4}
D-TPE-ASP/PDI (22.5μM)	12.38×10^{-4}	L-TPE-ASP/PDI (22.5μM)	-5.32×10^{-4}
495 nm			
D-TPE-ASP/PDI (2.25μM)	-6.32×10^{-3}	L-TPE-ASP/PDI (2.25μM)	3.05×10^{-3}
D-TPE-ASP/PDI (22.5μM)	-3.41×10^{-3}	L-TPE-ASP/PDI (22.5μM)	2.43×10^{-3}

Tab. S5 g_{lum} of TPE-ASP/PDI in H_2O-DIOX (9/1; V/V)

460 nm			
D-TPE-ASP	-2.32×10^{-2}	L-TPE-ASP	1.45×10^{-2}
D-TPE-ASP/PDI (2.25 μM)	-2.41×10^{-2}	L-TPE-ASP/PDI (2.25 μM)	1.71×10^{-2}
D-TPE-ASP/PDI (22.5 μM)	-2.19×10^{-2}	L-TPE-ASP/PDI (22.5 μM)	1.59×10^{-2}
550 nm			
D-TPE-ASP	-1.82×10^{-2}	L-TPE-ASP	0.96×10^{-2}
D-TPE-ASP/PDI (2.25 μM)	-1.62×10^{-2}	L-TPE-ASP/PDI (2.25 μM)	0.85×10^{-2}
D-TPE-ASP/PDI (22.5 μM)	-1.01×10^{-2}	L-TPE-ASP/PDI (22.5 μM)	0.46×10^{-2}
595 nm			
D-TPE-ASP	-1.56×10^{-2}	L-TPE-ASP	0.86×10^{-2}
D-TPE-ASP/PDI (2.25 μM)	-0.94×10^{-2}	L-TPE-ASP/PDI (2.25 μM)	0.80×10^{-2}
D-TPE-ASP/PDI 22.5 μM)	-0.8×10^{-2}	L-TPE-ASP/PDI (22.5 μM)	0.19×10^{-2}

Tab. S6 The specific rotation of D/L-ASP

Specific Rotation [α]		
	L-ASP	**D-ASP**
[α]	4.2	-4.8
	4.3	-5.2
	4.5	-4.9
	4.5	-5.1
	4.6	-4.7
	4.5	-5.0
	4.3	-4.9
	4.4	-5.0
	4.6	-4.7
Average	4.43	-4.92
ee	88.6%	98.4%

Enantiomeric excess value of raw material ASP

According to the Eq. S3[1, 2]:

$$\mathbf{ee}=\frac{[\alpha]}{[\alpha]_{Pure}}\times\mathbf{100\%} \qquad \mathbf{S3}$$

References:

1 Neuberger, Adv Protein Chem Struct Biol., 1948, 4, 297-383.

2 Simona Rossi, Pierandrea Lo Nostro, Marco Lagi, Barry W. Ninham and Piero Baglioni, J. Phys. Chem. B, 2007, 35, 10510-10519.